A Computational Study of Nicotine Conformations in the Gas Phase and in Water

Donald E. Elmore and Dennis A. Dougherty*

Division of Chemistry and Chemical Engineering, California Institute of Technology, Pasadena, California 91125

Received September 1, 1999

The conformational preferences of nicotine in three protonation states and in the gas phase as well as aqueous solution are investigated using several computational procedures. Conformational aspects emphasized are *N*-methyl stereochemistry, relative rotation of the pyridine and pyrrolidine rings, and pyrrolidine ring conformation. All methods consistently predicted that the *N*-methyl trans species are most stable for all protonation states in both gas phase and in water. However, the cis/trans energy gap is significantly reduced in water. Additionally, the two pyridine ring rotamers, which are energetically equivalent in the gas phase, experience different solvation energies in water.

Introduction

Nicotine (Figure 1) is a major drug of abuse, acting as a potent agonist of the nicotinic acetylcholine receptor (nAChR). In addition, nicotinic agonists and antagonists have recently been identified as promising therapeutic targets for a variety of conditions including the treatment of pain, cognitive and attention deficits, Parkinson's disease, Tourette's syndrome, anxiety, and, of course, smoking cessation.[1] A thorough understanding of the geometric and electronic structure of nicotine is clearly essential in efforts to elucidate receptor structure and function or design new pharmaceuticals. Several early experimental and theoretical studies investigated the relative stabilities of different nicotine conformers.[2−11] Much of this work focused on three conformational aspects of nicotine: the position of the N8-methyl substituent relative to the pyridine ring (cis or trans); the relative orientation of the two rings; and the conformation of the pyrrolidine ring. Crystal structures of both the monoprotonated and diprotonated forms of nicotine as iodide salts have been obtained.[2] These structures showed the two rings nearly perpendicular to one another and a trans N8-methyl group. In general, of course, crystal structures do not give direct insight into the relative conformer populations present in solution. In addition, the crystals for the diprotonated and physiologically relevant monoprotonated species were grown from ethanol, in which nicotine might adopt a different conformation than in water. Other experimental work has been performed to probe solution phase nicotine conformations.[3−8] An early NMR NOE study proposed that the N8-methyl group was cis to the phenyl ring.[3] Later NMR studies by Whidby and Seeman refuted this conclusion and estimated an approximately 10:1 trans/cis ratio of nicotine at equilibrium, corresponding to a free energy difference of about 1.4 kcal/mol at 25 °C.[4] This latter study was conducted at very low pH in order to suppress N8-inversion and thus involved characterization of the nonphysiological diprotonated form. As a result, conclusions concerning the physiologically relevant monoprotonated form were necessarily indirect. Further NMR structural studies proposed that the pyridine and pyrrolidine rings are approximately perpendicular to one another and that the pyrrolidine ring adopts an envelope conformation with the N8 atom out of plane.[5] However, these NMR studies were performed using a $CDCl_3/CFCl_3$ solvent mixture, which could lead to different conformational stabilities than aqueous solvent.

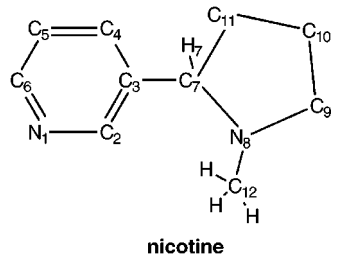

Figure 1. Numbering scheme used for nicotine and related species in this work.

Previous computational studies of nicotine conformation employed PCILO,[9] molecular mechanics,[10] INDO,[6,11] AM1,[12] and extended Hückel[13] methods. These studies generally produced results similar to those found in the NMR solution studies, with the N8-methyl group trans and the two rings approximately perpendicular to one

(1) For introductions to nicotine pharmacology and the interest in nicotinic agonists and antagonists, see: Bannon, A. W., et al. *Science* **1998**, *279*, 77−81. Holladay, M. W.; Dart, M. J.; Lynch, J. K. *J. Med. Chem.* **1997**, *40*, 4169−4194. Elgen, R. M.; Hunter, J. C.; Dray, A. *Trends Pharm. Sci.* **1999**, *20*, 337−342.

(2) (a) Barlow, R. B.; Howard, J. A. K.; Johnson, O. *Acta Crystallogr.* **1986**, *C42*, 853−856. (b) Koo, C. H.; Kim, H. S. *Daehan Hwahak Hwoejee* **1965**, *9*, 134−141. Koo, C. H.; Kim, H. S. *Chem. Abstr.* **1966**, *64*, 6431e.

(3) Chynoweth, K. R.; Ternai, B.; Simeral, L. S.; Maciel, G. E. *Mol. Pharmacol.* **1973**, *9*, 144−151.

(4) Whidby, J. F.; Seeman, J. I. *J. Org. Chem.* **1976**, *41*, 1585−1590.

(5) Pitner, T. P.; Edwards, W. B., III; Bassfield, R. L.; Whidby, J. F. *J. Am. Chem. Soc.* **1978**, *100*, 246−251.

(6) Seeman, J. I. *Heterocycles* **1984**, *22*, 165−193.

(7) Whidby, J. F.; Edwards, W. B., III; Pitner, T. P. *J. Org. Chem.* **1979**, *44*, 794−798.

(8) Cox, R. H.; Kao, J.; Secor, H. V.; Seeman, J. I. *J. Mol. Struct.* **1986**, *140*, 93−106.

(9) Pullman, B.; Courrière, P.; Coubeils, J. L. *Mol. Pharmacol.* **1971**, *7*, 397−405.

(10) Hacksell, U.; Mellin, C. *Prog. Brain Res.* **1989**, *79*, 95−100.

(11) Radna, R. J.; Beveridge, D. L.; Bender, A. L. *J. Am. Chem. Soc.* **1973**, *95*, 3831−3842.

10.1021/jo991383q CCC: $19.00
Published on Web 01/20/2000

another. All of these calculations involved levels of theory well below the current state of the art. In addition, they were conducted in the gas phase, ignoring possible effects arising from interactions with water. Recently, more modern computational techniques have been used to study the conformations of other nAChR ligands: ACh,[14] epibatidene,[15] and anatoxin-a,[16] and it thus seemed appropriate to perform a comparable study on nicotine.

Here, we report high-level quantum mechanical studies of nicotine in the gas phase. In addition, two very different water solvation models have been used to evaluate relative stabilities in aqueous media. The first is an explicit solvent model using TIP4P and the OPLS force field developed and applied by Jorgensen[17] along with Monte Carlo (MC) statistical perturbation theory (SPT) methods. SPT/OPLS methods have been used to calculate solvent effects for a variety of chemical systems, including heterocycles similar to nicotine, such as *N*,*N*′-diphenylguanidinium, histamine, nicotinic and isonicotinic acids, and pyrrole and imidazole.[18] (For a review of different MC free energy calculations and their applications, see ref 19.) Our second solvation model is a quantum mechanical, continuum method developed recently by Cramer and Truhlar (SM5.42R).[20] This method has been parametrized for a number of HF and DFT methods, and three of these parametrizations were employed in this study. The method has produced good results across a wide range of solutes, and it has been shown to work well for N-containing species, which are sometimes problematic for solvation methods.

The various levels of theory employed consistently predict that trans species are more stable than cis species for the physiologically relevant singly protonated nicotine, as well as for other possible protonation states in both the gas phase and water. Additionally, calculated relative ΔG_{sol} values imply that the two possible rotamers of each nicotine stereoisomer have different solvation behaviors.

Computational Methods

Gas-Phase Calculations. All AM1 and MMFF94 calculations were performed using the SPARTAN 5.0 software package,[21] and all ab initio and density functional theory (DFT) calculations were performed using the Gaussian 94 suite of programs.[22] Six species were considered in this study: the cis and trans stereoisomers of unprotonated (0), singly protonated (+), and doubly protonated (++) nicotine. Depictions of the + forms of these isomers are shown in Figure 2; analogous structures were considered for the other protonation states. Two sources of conformational uncertainty in these molecules were investigated: rotation around the C3−C7 bond and pyrrolidine ring conformations. An initial survey of ring rotation conformers was obtained from AM1 and MMFF94 rotational profiles, which produced two conformational minima, **A** and **B** (Figure 3). Optimized structures for the two rotational minima (**A** and **B**) of each species were then obtained at the HF/6-31G** level. Frequency calculations were performed on HF/6-31G**-optimized structures to verify structures were true minima, and CHELPG charges[23] were obtained from the HF/6-31G** wave function. The frequency calculations also yielded estimates of the thermal energy (TE) and entropy (*S*) of the species at 298 K and 1 atm. Single-point energies were obtained for optimized species at the MP2/6-31G** and B3LYP/6-31G** levels. ΔG values were determined at each computational level in the following manner: $\Delta G = \Delta E + \Delta TE - 298(\Delta S)$, where ΔE was obtained at several levels of theory, while ΔTE and ΔS always were derived from the HF/6-31G** frequency calculations. Although the internal energy, thermal energy, and entropy of the structures were only calculated in the gas phase, these values should provide valid estimates for the solvated species. The ΔG due to solute−solvent interactions, estimated by solvation calculations, should dominate changes in the solute entropy and thermal energy resulting from solvation. This technique of combining gas phase ΔG estimates with ΔG_{solv} estimates from SPT calculations has been successfully applied to other systems.[18,19]

Solvation Calculations. Explicit OPLS/SPT calculations were performed using BOSS version 3.8[24] on the physiologically important singly protonated (+) **A** and **B** rotamers. HF/6-31G**-optimized geometries were used for the solute structures, which were kept rigid for each window of the SPT simulation. Calculations were performed with 500 TIP4P water molecules in a cubic cell approximately 25 Å on each side using the isothermic−isobaric ensemble (NPT) at 25 °C and 1 atm. Standard OPLS all atom Lennard−Jones parameters were used for the solute molecules, and CHELPG charges[23] fit to the HF/6-31G** wavefunction were used for solute atomic charges, as previously recommended.[25] Solvent−solvent and solute−solvent interactions were cut off at 12 and 10 Å, respectively, with potential functions quadradically feathered to zero over the final 0.5 Å. During each perturbation, the geometries, charges, and Lennard−Jones parameters were linearly scaled from the starting species ($\lambda = 0$) to the final species ($\lambda = 1$) using a coupling parameter λ. Double-wide sampling was performed to yield 20 simulation windows of $\Delta\lambda = 0.05$ each. For each window, 2×10^6 and 4×10^6 conformations were sampled for equilibrium and averaging phases, respectively. Volume moves were attempted every 1000 configurations, and solute moves were attempted every 50 configurations; ranges for these moves were set to allow approximately 40% of the moves to be accepted.

Continuum solvation calculations were performed using the SM5.42R model.[17] We employed the HF/6-31G*, HF/cc-pDVZ, and BPW91/6-31G* parametrizations of the SM5.42R method to obtain gas-phase internal energies and ΔG_{sol} energies for

(12) Berthelot, M.; Decouzon, M.; Gal, J.-F.; Laurence, C.; Le Questel, J.-V.; Maria, P.-C.; Tortajada, J. *J. Org. Chem.* **1991**, *56*, 4490−4494.
(13) Kier, L. B. *Mol. Pharmacol.* **1968**, *4*, 70−76.
(14) (a) Segall, M. D.; Payne, M. C.; Boyes, R. N. *Mol. Phys.* **1998**, *93*, 365−370. (b) Edvardsen, Ø.; Dahl, S. G. *J. Neural Transm.* **1991**, *83*, 157−170. (c) Margheritis, C.; Corongiu, G. *J. Comput. Chem.* **1988**, *9*, 1−10.
(15) Campillo, N.; Páez, J. A.; Alkorta, I.; Goya, P. *J. Chem. Soc., Perkin Trans. 2* **1998**, *2*, 2665−2669.
(16) Thompson, P. E.; Manallack, D. T.; Blaney, F. E.; Gallagher, T. *J. Comput. Aided Mol. Design* **1992**, *6*, 287−298.
(17) Jorgensen, W. L.; Maxwell, D. S.; Tirado-Rives, J. *J. Am. Chem. Soc.* **1996**, *118*, 11225−11236.
(18) (a) Nagy, P. I.; Durant, G. J. *J. Chem. Phys.* **1996**, *104*, 1452−1463. (b) Nagy, P. I.; Durant, G. J.; Hoss, W. P.; Smith, D. A. *J. Am. Chem. Soc.* **1994**, *116*, 4898−4909. (c) Nagy, P. I.; Takács-Novák, K. *J. Am. Chem. Soc.* **1997**, *199*, 4999−5006. (d) Nagy, P. I.; Durant, G. J.; Smith, D. A. *J. Am. Chem. Soc.* **1993**, *115*, 2912−2922.
(19) Jorgensen, W. L. *Acc. Chem. Res.* **1989**, *22*, 184−189.
(20) (a) Li, J.; Hawkins, G. D.; Cramer, C. J.; Truhlar, D. G. *Chem. Phys. Lett.* **1998**, *288*, 293−298. (b) Zhu, T.; Li, J. B.; Hawkins, G. D.; Cramer, C. J.; Truhlar, D. G. *J. Chem. Phys.* **1998**, *109*, 9117−9133.
(21) SPARTAN version 5.0. Wavefunction, Inc., 18401 Von Karman Ave., Suite 370, Irvine, CA 92612.
(22) Gaussian 94. Gaussian 94, Revision D.3: Frisch, M. J.; Trucks, G. W.; Schlegel, H. B.; Gill, P. M. W.; Johnson, B. G.; Robb, M. A.; Cheeseman, J. R.; Keith, T.; Petersson, G. A.; Montgomery, J. A.; Raghavachari, K.; Al-Laham, M. A.; Zakrzewski, V. G.; Ortiz, J. V.; Foresman, J. B.; Cioslowski, J.; Stefanov, B. B.; Nanayakkara, A.; Challacombe, M.; Peng, C. Y.; Ayala, P. Y.; Chen, W.; Wong, M. W.; Andres, J. L.; Replogle, E. S.; Gomperts, R.; Martin, R. L.; Fox, D. J.; Binkley, J. S.; Defrees, D. J.; Baker, J.; Stewart, J. P.; Head-Gordon, M.; Gonzalez, C.; Pople, J. A. Gaussian, Inc., Pittsburgh, PA, 1995.
(23) Breneman, C. M.; Wiberg, K. B. *J. Comput. Chem.* **1990**, *11*, 361−373.
(24) BOSS Version 3.8. Jorgensen, W. L. Department of Chemistry, Yale University, P.O. Box 208107, New Haven, CT 06520-8107.
(25) Carlson, H. A.; Nguyen, T. B.; Orozco, M.; Jorgensen, W. L. *J. Comput. Chem.* **1993**, *14*, 1240−1249.

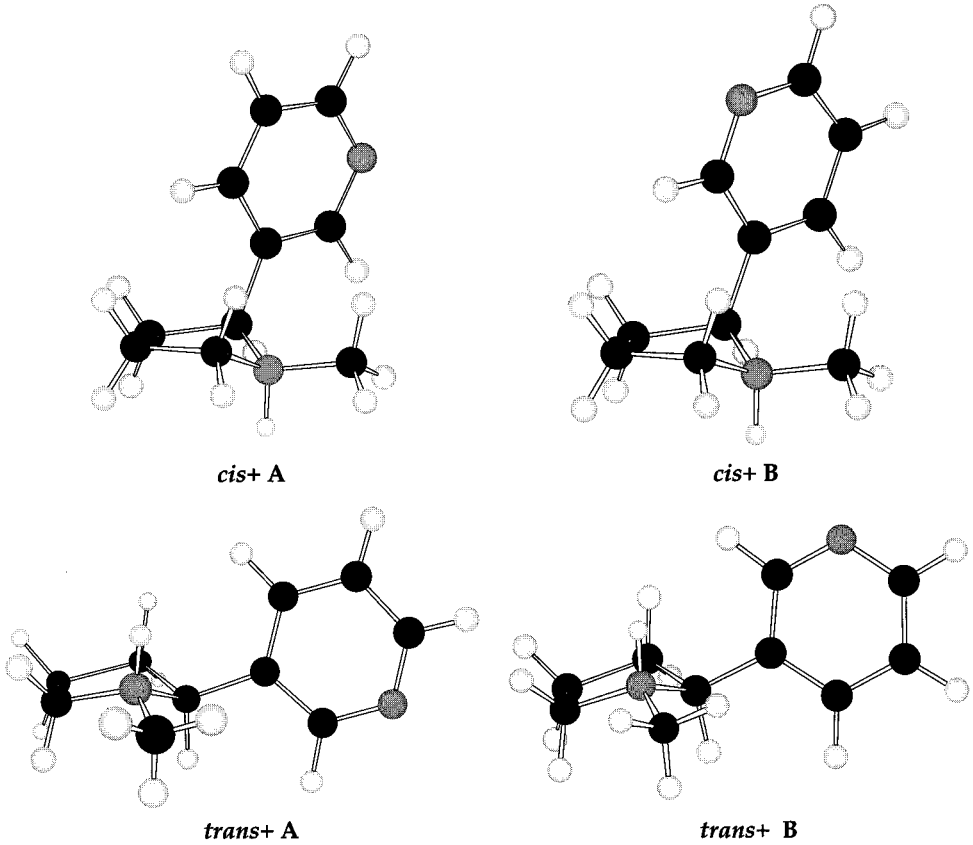

Figure 2. Three-dimensional structures of the singly protonated (+) nicotine species considered computationally optimized at the HF/6-31G** level. C atoms are shown in black, N atoms in gray, and H atoms in white.

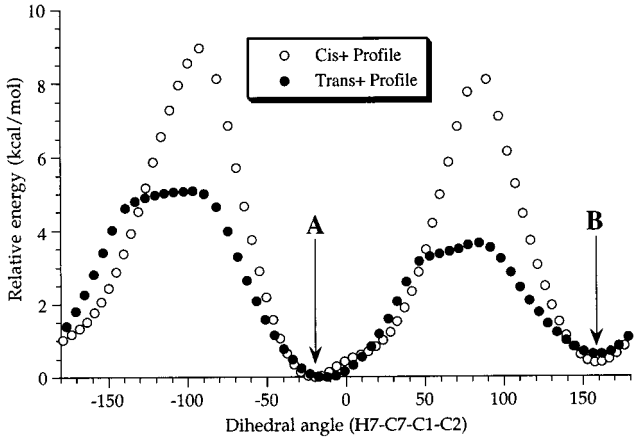

Figure 3. Rotational profiles of singly protonated nicotine species determined using the MMFF94.

the **A** and **B** rotamers of all structures. Rigid HF/6-31G** geometries were used for these calculations, and gas-phase thermal energy and entropy estimates were taken from HF/6-31G** calculations. All SM5.42R calculations will be noted as follows: level of SM5.42R parametrization used for *E* and ΔG_{sol}//level of theory used to optimize solute geometry. The more rigorous SCF convergence method (ISCRF = 1) was used for these calculations.

Results and Discussion

Rotational Profiles around the C3−C7 Bond. Previous experimental results and computations had predicted the presence of two rotamers, both of which have the pyridine and pyrrolidine rings of nicotine roughly perpendicular to one another, for the cis and trans species.[5,9,10,13] The presence of these two rotamers was confirmed by calculating AM1 and MMFF94 rotational profiles for each species. MMFF94 profiles for the singly protonated species (+) are shown in Figure 3, and similar profiles were obtained using AM1, as well as for the other protonation states. The two rotamers, labeled **A** and **B**, have dihedral H7−C7−C3−C2 close to 0° and 180°, respectively. Rotational barriers between the two predicted rotamers are not large—generally about 3 kcal/mol for trans configurations and 6−8 kcal/mol for cis configurations regardless of protonation state. This is consistent with increased steric interactions between the N8-methyl group and the pyridine ring in the cis species.

Gas-Phase Structures. Gas-phase optimized structures were calculated for the **A** and **B** rotamers of all species at the HF/6-31G** level. Although the major contributors in aqueous solution may not all be detectable as gas-phase minima,[26] this seems unlikely in the present system, which has relatively few degrees of conformational freedom. Selected geometric quantities for these structures are given in Table 1. The two rings remain nearly perpendicular to one another, as seen by the H7−C7−C3−C2 dihedral angles. Similar relative ring orientations were also predicted by previous calculations[9,10,13] and NMR studies;[5] crystal structures of the + and ++ structures showed an **A** conformation.[2] The intramolecular N3−N8 distances are interesting to note. The **A** rotamers place the two N atoms farther apart than the **B** rotamers for all species, which is likely important in rotamer solvation differences noted below. This N−N

(26) Colominas, C.; Luque, F. J.; Orozco, M. *J. Phys. Chem. A* **1999**, *103*, 6200−6208.

Table 1. Selected Geometric Attributes of Nicotine Species Optimized at the HF/6-31G Level[a]**

species	N1−N8	H7−C7−C3−C2	N8−C9−C10−C11	C9−C10−C11−C7
cis+ **A**	4.582	−19.0	−18.5	−6.7
cis+ **B**	4.529	159.8	−18.8	−6.2
trans+ **A**	4.655	−5.9	1.3	23.3
trans+ **B**	4.385	178.0	4.0	21.0
cis **A**	4.633	−18.9	−16.9	−6.9
cis **B**	4.537	160.6	−17.4	−6.4
trans **A**	4.793	16.5	25.7	−1.4
trans **B**	4.247	−164.7	25.6	−1.2
cis++ **A**	4.749	−5.6	−41.0	40.5
cis++ **B**	4.708	140.7	−22.3	40.5
trans++ **A**	4.737	1.7	7.6	17.8
trans++ **B**	4.546	162.6	−1.5	26.0

[a] Distances are in Å and all angles are in degrees. Pyrrolidine dihedral angles are given in the last two columns.

distance difference between rotamers is more pronounced in trans than cis species. Also, the N−N distance increases between + and ++ species, as the two positively charged N atoms apparently repel each other; this also has been observed in crystal structures.[2]

Pyrrolidine ring conformation has been ambiguous in previous work. NMR studies on nicotine and closely related compounds have implied that the ring has an envelope conformation with the N atom out of plane.[5−7] However, this NMR data was obtained in nonaqueous solution, so the nonprotonated species (0) would have been present. Conversely, the mono- and diprotonated crystal structures show species with more twisted conformations.[2] Several ring conformations were considered here for each of the species, and the most stable conformers found are presented in Table 1. As in the NMR work, the trans0 species has the envelope conformation for the pyrrolidine ring with the N atom out of plane. However, upon protonation, the trans+ and trans++ species alter their envelope conformation to place the C7 atom out of plane, which is different than the conformations seen in crystal structures of these species[2]. All cis0 and cis+ structures have similar conformations, with the N8-atom out of plane, although the C7, C9, C10, and C11 atoms are slightly less planar than in trans0 conformers. Doubly protonated cis++ **A** and **B** structures show conformations different from other protonation states with C10 and C11 out of plane, respectively.

Gas-Phase Energetics. Energetic comparisons of the four nicotine conformers were performed using several different levels of theory (HF/6-31G**, MP2/6-31G**//HF/6-31G**, and B3LYP/6-31G**//HF/6-31G**) as shown in Table 2. ΔG values along with the correction from HF/6-31G** frequency calculations used to calculate ΔG from ΔE (described in methods section) are given. As can be seen, ΔG values predict a larger energy gap between cis and trans stereoisomers than ΔE values. This is because trans species have a more favorable entropy, calculated to be more than 3 cal/mol K greater than for cis in the + state. The effect persists, but is smaller for the 0 and ++ species. It seems reasonable that trans species are entropically favored over the more compact and restricted cis molecules.

Generally, the agreement among the predictions of the three methods is quite good, with only relatively minor, quantitative differences evident. At all computational levels, trans species are predicted to be more stable than the cis ones for all protonation states, consistent with expectations based on sterics. Little difference is predicted between the A/B rotamers in any of the structures. This disagrees with PCILO and INDO results, which predicted rotamer energy differences of around 1 kcal/mol.[9,11] Interestingly, the 0 and ++ species, especially the trans stereoisomers, show larger energy gaps between rotamers.

Table 2. Relative Gas-Phase ΔG Values and Thermal Energy and Entropy Corrections for All Nicotine Species Considered[a]

species/conformer	HF/6-31G** ΔG values	MP2/6-31G**//HF/6-31G** ΔG values	B3LYP/6-31G**//HF/6-31G** ΔG values	ΔTE + 298(ΔS) relative to trans **A**
cis+ **A**	4.32	2.87	4.09	1.19
cis+ **B**	4.38	2.94	4.15	1.24
trans+ **A**	0.00	0.00	0.06	0.00
trans+ **B**	0.00	0.01	0.00	−0.03
cis **A**	5.21	4.30	4.83	0.67
cis **B**	5.44	4.53	5.08	0.73
trans **A**	0.00	0.00	0.00	0.00
trans **B**	0.48	0.52	0.44	−0.04
cis++ **A**	3.41	2.51	2.69	0.23
cis++ **B**	3.60	2.75	3.18	0.18
trans++ **A**	0.00	0.00	0.00	0.00
trans++ **B**	1.03	1.07	1.03	0.07

[a] All values are given in kcal/mol.

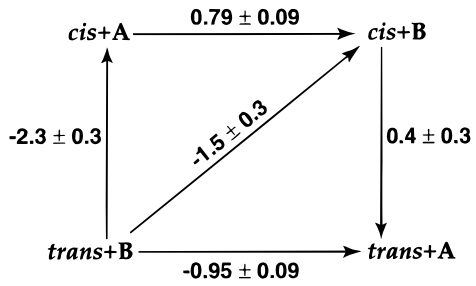

Figure 4. Thermodynamic cycle of $\Delta\Delta G_{sol}$ values determined from SPT/OPLS calculations on singly protonated nicotine species. All values are given in kcal/mol.

Solvation of the Physiologically Important Singly Protonated Species. An explicit solvent model using SPT was utilized to obtain relative free energies of solvation for the nicotine conformers, and a thermodynamic cycle for these simulations is shown in Figure 4. Cis+ **A** to trans+ **B** and cis+ **B** to trans+ **A** perturbations were performed, as the **A** rotamer of cis is in some aspects more spatially similar to the trans **B** rotamer. One "diagonal" simulation between trans+ **B** and cis+ **B** was also performed to verify the values obtained for other legs. These $\Delta\Delta G_{sol}$ values from the SPT/OPLS method can then be combined with calculated gas phase ΔG values (Table 2) to determine relative ΔG values for each of the + conformers (Table 3).

The SM5.42R method was also applied to the singly protonated conformers using the HF/6-31G*, HF/cc-pVDZ, and BPW91/6-31G* parametrizations with the gas-phase HF/6-31G**-optimized structures. Table 3 lists overall relative ΔG values for the species considering both gas-phase energies and solvation energies, along with the thermal energy and entropy estimates from HF/6-31G** gas-phase frequency calculations. As can be seen, SM5.42R $\Delta\Delta G_{sol}$ values are not identical in magnitude to those predicted using the SPT/OPLS method (Figure 4). Most

Table 3. Relative Δ*G* of Singly Protonated Species Including Computed Solvation Effects from SPT/OPLS and SM5.42R Calculations[a]

	SPT/OPLS			SM5.42R		
species/ conformer	HF/6-31G**	MP2/6-31G**// HF/6-31G**	B3LYP/6-31G**// HF/6-31G**	HF/6-31G*// HF/6-31G**	HF/cc-pVDZ// HF/6-31G**	BPW91/6-31G*// HF/6-31G**
cis+ **A**	3.1 ± 0.3	1.6 ± 0.3	2.8 ± 0.3	3.68	3.28	3.44
cis+ **B**	4.0 ± 0.3	2.5 ± 0.3	3.7 ± 0.3	3.81	4.01	3.58
trans+ **A**	0.0	0.0	0.0	0.00	0.00	0.00
trans+ **B**	0.95 ± 0.09	0.96 ± 0.09	0.89 ± 0.09	0.22	0.21	0.11

[a] All values are given in kcal/mol. First three data columns are from SPT/OPLS calculations; last three data columns are from SM5.42R.

Table 4. Predicted Relative Percentages of Singly Protonated Nicotine Species Present in Aqueous Solution at 25 and 37 °C (in Parentheses) Using Various Computational Methods[a]

species/ conformer	MP2/6-31G**// HF/6-31G** (SPT/OPLS)	B3LYP/6-31G**// HF/6-31G** (SPT/OPLS)	HF/6-31G*// HF/6-31G** (SM5.42R)	HF/cc-pVDZ// HF/6-31G** (SM5.42R)	BPW91/6-31G*// HF/6-31G** (SM5.42R)
cis+ **A**	5.3 (5.8)	0.8 (0.9)	0.1 (0.1)	0.2 (0.3)	0.2 (0.2)
cis+ **B**	1.1 (1.2)	0.2 (0.2)	0.1 (0.1)	0.1 (0.1)	0.1 (0.2)
trans+ **A**	78.1 (76.7)	81.0 (80.0)	59.0 (58.6)	58.7 (58.3)	54.6 (54.4)
trans+ **B**	15.5 (16.3)	18.1 (18.9)	40.8 (41.1)	41.0 (41.3)	45.1 (45.3)

[a] Since the entropy and thermal energy calculations considered structures at 25 °C, there is some additional uncertainty in the values for 37 °C.

strikingly, the trans+ **B**/cis+ **A** difference is −2.3 ± 0.3 kcal/mol from SPT/OPLS (Figure 4), while it is only between −0.889 and −1.382 using SM5.42R methods. Nevertheless, both methods predict the same order of ΔG_{sol} values for these conformers: (from most to least stabilizing) cis+ **A**, cis+ **B**, trans+ **A**, trans+ **B**. The two solvation models also lead to the same prediction of the overall most stable species, trans+ **A** (Table 3).

Both solvation models show two trends in ΔG_{sol} for these species: (1) cis species solvate better than trans, and (2) **A** rotamers solvate better than **B**. The cis/trans difference can be explained by considering the solvent accessible surface area (SASA) of the molecules, which can be determined using BOSS.[24] The cis species have a lower SASA (381 Å^2) than the trans (397 Å^2) and, therefore, reduce the unfavorable interactions that occur at the interface of the hydrophobic portions of the solute and water. In addition, the cis exposes the N^+−H more fully, and this is presumably the substructure that is best solvated by water. It may be that the explicit solvation model is better suited to predict this interaction. Analysis of radial distribution functions of water oxygen atoms around the N^+−H proton show that the first solvation shell has a similar population in cis and trans species. The solvation difference appears to arise because the second shell is held somewhat closer in the cis species, which may explain why the OPLS/SPT method predicts a larger cis/trans $\Delta\Delta G_{sol}$ than SM5.42R.

The **A** rotamers are possibly more stable because they have a larger separation between the two oppositely charged regions than in the **B** rotamers, leading to better solvation. Since this change in N−N distance is slightly larger between the trans+ than the cis+ rotamers, it is reasonable that the relative stabilization of the **A** rotamer is slightly larger in the trans+ species for almost all models.[27]

Comparisons of Overall Stabilities. These calculations involving different ab initio and solvation methods allow some clear predictions about the relative amounts of nicotine species present in aqueous solution. The overall Δ*G* values for the species lead directly to predicted equilibrium ratios of each species in solution using a Boltzmann distribution, as given for the singly protonated species at 25 °C and 37 °C in Table 4. Although the quantitative ratios show some dependence on the methods employed, all methods clearly predict that no more than 6% of the species should be in a cis conformation, even at the higher physiological temperature (37 °C). These results imply that the experimental 1:10 cis/trans ratio[4] may represent an upper limit of the amount of cis present. As well, in a receptor binding site, which is not purely aqueous, one would expect the relative proportion of cis to be lower than in bulk water. In addition, **A** and **B** rotamers, despite their near-degeneracy in the gas phase for + species, are predicted to differ in energy after considering solvation. These percentages do emphasize one difference between the predictions made by the two solvent methods used, as the SPT/OPLS methods predict that mainly trans+ **A** would be present while SM5.42R calculations predict that the amounts of trans+ **A** and **B** present at equilibrium would be more nearly equal.

These predictions of nicotine conformation can be considered in light of previous work attempting to predict the activity of nicotine analogues. Some previous studies have attempted to estimate the geometrical relationship between different "pharmacophore" groups important for nicotine binding, including estimates of optimal N−N distances. Earlier work proposed a N−N distance of 4.8 Å,[28] and the trans+ **A** N−N distance (4.655 Å) is quite close to this value. Later work considering the high-affinity nAChR ligand epibatidine has proposed a longer optimal N−N distance of 5.5 Å.[29] Although this estimate

(27) Calculation of ΔG_{sol} of the other nicotine protonation states (neutral and doubly protonated) was performed using the SM5.42R HF/6-31G* parametrized model on HF/6-31G** geometries. This model was applied to these systems in lieu of SPT/OPLS simulations because it produced similar qualitative trends for the singly protonated species at a fraction of the computational expense. The same cis/trans solvation trend seen for + species was seen for other protonation states, and trans species are still predicted to be most stable in aqueous solution. But interestingly, the **B** rotamers for both 0 and ++ species showed better solvation than the **A** ones. Thus, in species where the N atoms carry a similar charge, solvation appears to improve with decreased N−N distance.

(28) Sheridan, R. P.; Nilakantan, R.; Dixon, J. S.; Venkataraghavan, R. *J. Med. Chem.* **1986**, *29*, 899−906.

(29) Glennon, R. A.; Herndon, J. L.; Dukat, M. *Med. Chem. Res.* **1994**, *4*, 461−473.

is significantly longer than the trans+ **A** N−N distance, the trans+ **A** conformer does have the maximum N−N distance seen in the structures we considered in this work (Table 1). Additional research on conformationally restricted nicotine analogues, such as those described in recent reviews, may give insight into the physiological difference between the rotamers considered.[30]

In summary, a range of modern computational methodologies has been applied to nicotine in the gas phase and in solution. For the monoprotonated species all methods predict a substantial preference for the trans isomer. However, two conformers of trans nicotine (**A** and **B**) are expected to be significantly populated in aqueous media.

(30) Glennon, R. A.; Dukat, M. *Med. Chem. Res.* **1996**, *6*, 465−486.

Acknowledgment. We gratefully acknowledge Dr. Jiabo Li, Professor Christopher Cramer, and Professor Donald Truhlar of the University of Minnesota for providing the Gaussian Solvation Module and for many helpful discussions. Justin P. Gallivan (Caltech) also provided valuable assistance. D.E.E. is an NSF Predoctoral Fellow. This work was supported by NIH (NS 34407).

Supporting Information Available: Cartesian coordinates and total energies of HF/6-31G** optimized structures. This information is available free of charge via the Internet at http://pubs.acs.org.

JO991383Q